2021 9th International Conference on Control, Mechatronics and Automation (ICCMA) | 978-1-6654-1073-1/21/$31.00 ©2021 IEEE | DOI: 10.1109/ICCMA54375.2021.9646186

Pressure and Volume Control of a Non-invasive Mechanical Ventilator: a PI and LQR Approach

Sergio Morales[1,5], Styven Palomino[1,5], Ricardo Terreros[1,5], Victor Ulloque[2,5], Noé Bazán-Lavanda[6]
María Palacios-Matos[6], Julio Valdivia-Silva[3,4,5], Emir. A Vela[2,4,5] and Ruth Canahuire[1,4,5]
[1]Department of Electrical and Mechatronics Engineering, [2]Department of Mechanical Engineering,
[3]Department of Bioengineering, [4]Centro de Investigación en Bioingenieria - BIO
[5]Universidad de Ingenieria y Tecnologia - UTEC, [6]Alta Engineering SAC - AE, Lima - Peru
Email: {rcanahuire, evela, jvaldivias}@utec.edu.pe, {noe.bazan, mppalaci}@altaingsac.com

***Abstract*—Many studies in recent years have been focused on treating diseases caused by the SARS-CoV-2 virus, such as the Covid-19 disease. In this regard, the development of mechanical ventilation systems became very important for the care of patients with moderate symptoms caused by the virus. Most of the works developed used the non invasive mechanical ventilation system, since this is rapidly assembled and replicated. This work is centered on automating the manual Bag-Valve-Mask (BVM) ventilation of the Emergency Mechanical Ventilator for ICU (UTEC-AE EMV-ICU). For this purpose, it is necessary to implement a satisfactory control system to reach the adequate volume or pressure for patients. The control system implemented for the UTEC-AE EMV-ICU is based on LQR method for the three non-invasive ventilation modes (volumen controlled ventilation, pressure controlled ventilation, and assisted ventilation). The LQR control system of the UTEC-AE EMV-ICU was tested in an artificial lung where the obtained results were compared and discussed with the obtained results from a PI control system.**

***Index Terms*—Covid-19, Mechanical ventilator, non-invasive ventilation, LQR controller, PI controller**

I. Introduction

Since 2019, the world has been affected by the global pandemic due to the SARS-CoV-2 virus, occasioning on the Covid-19 disease. At present, this disease has caused around 4.5 million deaths worldwide [1], where the most affected were the developing countries located in Africa, Latin America, among others [2]. Many of these deaths are caused by acute respiratory failure that is why the virus is called SARS, severe acute respiratory syndrome [3]. Consequently, 10-20 % of all infected patients require mechanical ventilation to endure the disease [4]. As a result, ventilators are crucial in the fight against covid-19. However, the main problem with developing countries is their poor health system, which habitually cannot provide enough mechanical ventilators for all infected patients.

The mechanical ventilators can be classified as non-invasive and invasive ventilation systems. The non-invasive ventilators are characterized because of it is necessary to set all parameters to guarantee the air flow desired. These ventilators use BVM (Bag Valve Mask) and provide assisted ventilation. On the other hand, the invasive ventilation consists of a more complex system composed of special sensors and actuators to provide high levels of air flows required by patient [5].

Currently, many authors have been presenting contributions in the development of mechanical ventilators that can be used as an alternative of solution to the shortage [6]. For example, in [7], the MIT E-Vent Team proposes a low-cost ventilator prototype that provides air to the patient through the BVM. In [8], the work proposes an automated system of the manual BVM process using industrial sensors and PLC to improve the reliability of the ventilator. Finally, in [5], the authors propose a much more compact and portable design that consists of compression of a plastic air tank.

This paper proposes the experimental implementation of an automatic mechanism of ventilation in the UTEC-AE EMV-ICU based on the patent pending before INDECOPI (The Peruvian National Institute for the Protection of the Consumer and Copyright) [9], and which is conformed by a two-vane mechanism to compress the Self-inflating Bag. The Linear Quadratic Regulator (LQR) method is used to reach the desired pressure and volume values on an artificial lung. Likewise, a PI control system is implemented in the mechanism of ventilation for comparison process in terms of levels of overshoot, settling time, and steady-state error.

II. Methodology

A. Structure

The ventilation structure used in this work (see Figure 1) is based on the resuscitation bag principle. It consists of a bag full of air with a desired oxygen concentration is compressed by a mechanism pushing the oxygen out of the bag and in direction of the ventilation circuit.

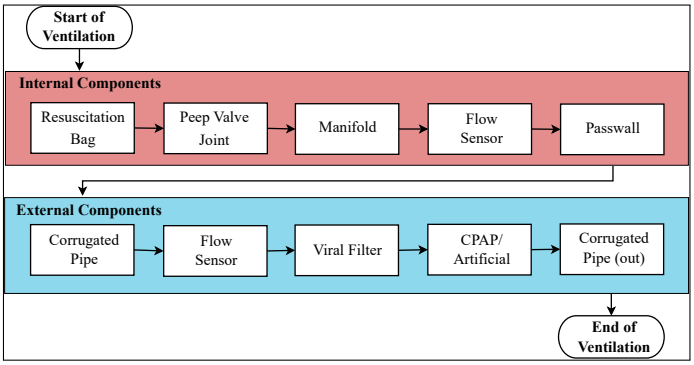

Fig. 1: Diagram of the mechanical ventilation circuit

The mechanism used in the UTEC-AE EMV-ICU for starting the oxygen flow (see Figure 2) is actioned by a DC motor with a planetary gearbox (188:1). The output shaft of the motor is coupled with a 30 tooth spur gear (diametral pitch, P_d = 16 and face width, F = 0.5 in), which transfers power to another two 48 tooth spur gears symmetrically aligned, forming an L with the pinion. The rotation of the first gear transfers torque to the other gears, generating movement to the two paddles that are attached to the shafts of the mechanism. These paddles compress the bag directing the air into the circuit. This gear coupling is achieved with the use of keys, keyseats, and keyways machined in the shafts, gears, and paddles. This prototype uses AISI 304 alloy for the mechanical parts and DURALUMINIO aluminum for the cover. Both transmission shafts have a $\frac{3}{4}$ in diameter and are placed in stainless steel rowlocks. Limit switches are used to detect the initial and final positions of the paddles, which are activated by being pushed by cams attached to the paddles (see Figure 2).

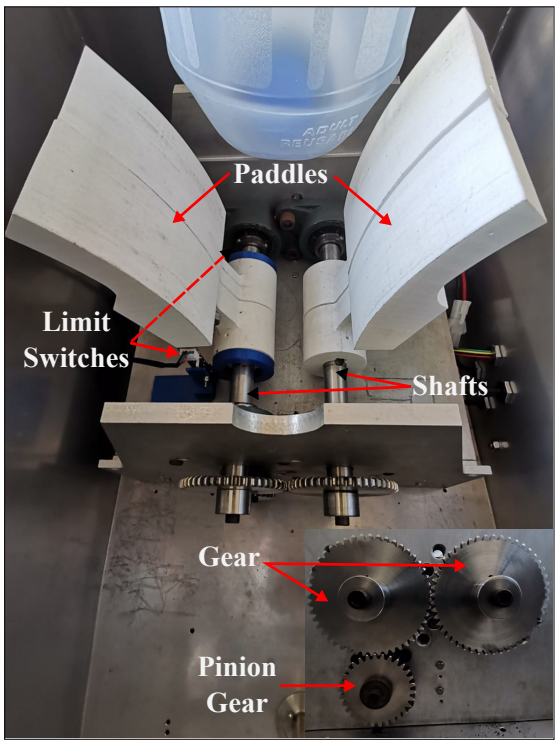

Fig. 2: Ventilation mechanism

B. Non-invasive Ventilation Modes

In non-invasive mechanical ventilation, monitoring and adjustment of parameters are necessary. Each patient requires different ventilation mode according to its needs; therefore, there are contrasting modes of operation for the non-invasive ventilator. In [10], all currently used operation modes are shown.

This work presents only two ventilation modes: control and assist-control. The first mode is used for pressure and volume, while the second mode is purely used for pressure support [11]. Each of these modes used is explained below.

- Pressure: In this control, the desired value is set for the pressure to achieve it whit the ventilator. The volume or flow is not taken into account since these parameters are generated as a product to reach the desired pressure. In addition, the pressure behavior is intended to be similar to a square wave.
- Volume: The idea is the same as for pressure, although, in this case, the desired parameter is the volume value. As well the values of pressure and flow are values necessary to reach the set volume.
- Pressure Suport: The ventilator uses this mode of operation when activated by the patient through the generation of negative pressure. Despite automatic activation, this one is an assisted control as it is also necessary to set the required parameters for the patient.

C. PI Controller

The PI controller is the most often used variation of the Proportional Integral Derivative (PID) controller, this variation only uses the proportional and integral terms. The proportional term proportionally increases the control effort with the error. It reduces the steady-state error but does not eliminate it, it also reduces the rise time but increments the overshoot. The Integral Term helps reduce the steady-state error, however it can make the system oscillate [12].

The block diagram of the Closed-Loop PI Control System is shown in Figure 3, where $r(t)$ is the desired output, $e(t)$ is the feedback error, $u(t)$ is the control effort and $y(t)$ is the actual output. In the mechanical ventilator system, $r(t)$ is the desired volume or the desired pressure, $u(t)$ is the PWM or the speed command sent to the motor driver and $y(t)$ is the measured volume or the measured pressure, being the former for the Volume Control and the latter for the Pressure Control or Pressure Support Control.

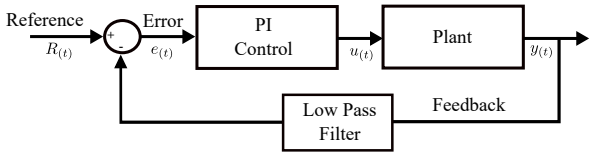

Fig. 3: Block Diagram of the PID controller.

The output of a PI controller, which is fed into the system as the manipulated variable input, is calculated in the time domain as follows [12]:

$$u(t) = K_p e(t) + K_i \int_0^t e(t)dt \tag{1}$$

The transfer function of the controller in the frequency domain is as follows:

$$K(s) = \frac{U(s)}{E(s)} = K_p + \frac{K_i}{s} \tag{2}$$

where K_p is the proportional gain and K_i is the integral gain. Both gains need to be tuned in order to meet the design requirements.

D. LQR Controller

The linear quadratic regulator (LQR) is a state feedback controller and is one of the most simple optimal controllers that can be developed, as it is easy to calculate its gains [13].

The block diagram of the LQR Control System is shown in Figure 4, where $\boldsymbol{r}(t)$ are the desired outputs, $\boldsymbol{x}(t)$ is the state vector, $\boldsymbol{K}$ is the state feedback control gain matrix, $\boldsymbol{e}(t)$ is the state feedback error vector and $u(t)$ is the control effort. In the mechanical ventilator system, $\boldsymbol{r}(t)$ are the desired volume and flow or the desired pressure and its derivative, $\boldsymbol{x}(t)$ contains the measured volume and flow or the measured pressure and its derivative and $u(t)$ is the PWM or the speed command sent to the motor driver, being the former for the Volume Control and the latter for the Pressure Control or Pressure Support Control.

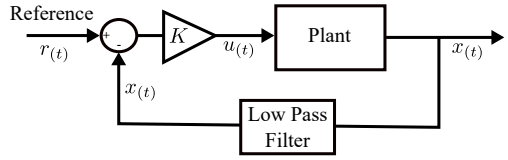

Fig. 4: Block Diagram of the LQR controller.

Given a linear system in state-space form:

$$\begin{aligned} \dot{\boldsymbol{x}} &= \boldsymbol{A}\boldsymbol{x} + \boldsymbol{B}u \\ y &= \boldsymbol{C}\boldsymbol{x} + \boldsymbol{D}u \end{aligned} \tag{3}$$

The controller propose the following cost function to minimize [14]:

$$\boldsymbol{J} = \int_0^\infty [\boldsymbol{x}^T \boldsymbol{Q}\boldsymbol{x} + \boldsymbol{u}^T \boldsymbol{R}\boldsymbol{u}]dt \tag{4}$$

where $\boldsymbol{Q}$ and $\boldsymbol{R}$ are positive-definite Hermitian matrices whose elements determine the relative importance of the error and the expenditure of the energy of the control signals [14]. The values of the elements of the matrices $\boldsymbol{Q}$ and $\boldsymbol{R}$ have to be chosen in order to meet the design requirements.

The gain matrix $\boldsymbol{K}$ is computed with following equation:

$$\boldsymbol{K} = \boldsymbol{R}^{-1}\boldsymbol{B}^T\boldsymbol{P} \tag{5}$$

where $\boldsymbol{P}$ is a positive-definite matrix which must satisfy the reduced-matrix Riccati equation [14]:

$$\boldsymbol{A}^T\boldsymbol{P} + \boldsymbol{P}\boldsymbol{A} - \boldsymbol{P}\boldsymbol{B}\boldsymbol{R}^{-1}\boldsymbol{B}^T\boldsymbol{P} + \boldsymbol{Q} = \boldsymbol{0} \tag{6}$$

Given the following matrix:

$$\boldsymbol{A_c} = \boldsymbol{A} - \boldsymbol{B}\boldsymbol{K} \tag{7}$$

where $\boldsymbol{A}$, $\boldsymbol{B}$, and $\boldsymbol{K}$ can be written as

$$\boldsymbol{A} = \begin{bmatrix} a_1 & a_2 \\ a_3 & a_4 \end{bmatrix}, \boldsymbol{B} = \begin{bmatrix} 0 \\ 1 \end{bmatrix}, \boldsymbol{K} = \begin{bmatrix} k1 & k2 \end{bmatrix}.$$

The state variables in steady-state can be calculated as:

$$\boldsymbol{x}(\infty) = -\boldsymbol{A_c}^{-1}\boldsymbol{B}\boldsymbol{K}\boldsymbol{r}_0 \tag{8}$$

where,

$$\boldsymbol{r}_0 = \begin{bmatrix} r_0 \\ 0 \end{bmatrix}$$

Solving the equation (8) gives:

$$\boldsymbol{x}(\infty) = \begin{bmatrix} \frac{a_2 k_1 r_0}{\det A_c} \\ \frac{-a_1 k_1 r_0}{\det \boldsymbol{A_c}} \end{bmatrix} \tag{9}$$

where $\det \boldsymbol{A_c}$ represents the determinant of the matrix $\boldsymbol{A_c}$.

Thus, equation (10) shows the compensation gain that needs to be used in order to allow the output signal to follow the reference (step signal).

$$G_c = \frac{\det \boldsymbol{A_c}}{a_2 k_1} \tag{10}$$

Finally, the control law of the LQR is defined as follows:

$$\hat{\boldsymbol{u}}(t) = \boldsymbol{K}\boldsymbol{e}(t) = \boldsymbol{K}(\boldsymbol{r}(t) - \boldsymbol{x}(t)) \tag{11}$$

and the input signal of the plant can be obtained as $\mathbf{u}(t) = G_c\hat{\mathbf{u}}(t)$.

III. Results

A. Low-Pass Filter

The low pass filter used in this work is a moving average with a finite impulse response. The moving average filter is commonly used with time series data to smooth short-term swings and highlight long-term trends or cycles. In this application, it is taken into account the weighted average of the previous 10 data points [15]. The filtered output signal is obtained as

$$y[n] = \frac{1}{M}\sum_{z=0}^{M-1} x[n-z]$$

where M is the number of data points (M = 10).

B. LQR and PI Control System

This section presents the comparison between the proposed LQR controller and a PI controller. This comparison aims to determine if the LQR controller has a better performance. Based on this, the settling time, overshoot, and steady-state error are analyzed in each of the three operation modes.

Figure 5 presents the response of the system for a ramp type reference of volume with a peak magnitude of 300 mL in both controllers.

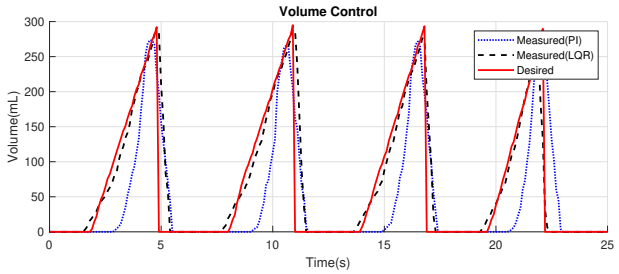

Fig. 5: PI vs LQR in volume control.

The gains for the volume PI controller are:

$$K_p = 0.15, K_i = 0.4$$

On the other hand, the gains for the volume LQR controller are:

$$\boldsymbol{K} = \begin{bmatrix} 0.3 & 0.7 \end{bmatrix}$$

The Table I shows some response characteristics of the system with both controllers. As can be seen, the LQR controller exhibits a better performance of the system with a less settling time and steady-state error, and no overshoot.

TABLE I: Comparison of system response in volume control

	Settling Time (s)	Overshoot (%)	S-S Error (%)
PI	1.5	7.4	18.5
LQR	0.8	0	6.3

It also can be seen in Figure 6 that the monitoring variables show better behavior with the LQR controller.

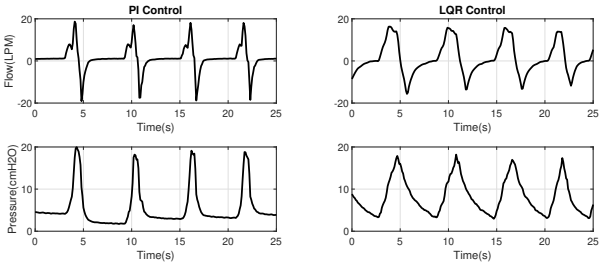

Fig. 6: Monitoring variables in volume control

Figure 7 presents the response of the system for a step type reference of pressure with a magnitude of 15 cmH2O in both controllers.

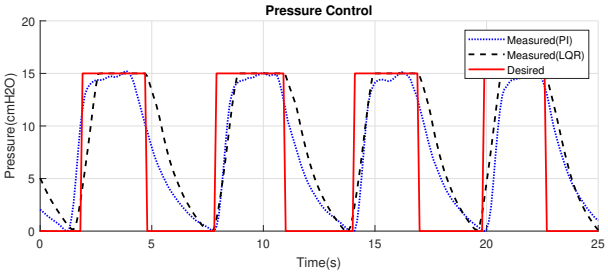

Fig. 7: PI vs LQR in pressure control.

The gains for the pressure PI controller are:

$$K_p = 40, K_i = 1$$

On the other hand, the gains for the pressure LQR controller are:

$$\boldsymbol{K} = \begin{bmatrix} 50 & 0.7 \end{bmatrix}$$

The Table II shows the same response characteristics of the system with both controllers. As can be seen, the LQR controller exhibits again a better performance of the system

TABLE II: Comparison of system response in pressure control

	Settling Time (s)	Overshoot (%)	S-S Error (%)
PI	0.75	1.3	4.5
LQR	0.7	0	0.2

with a less settling time and no overshoot nor steady-state error.

In this type of control, the monitoring variables show a slightly better behavior with the LQR controller as shown in Figure 8.

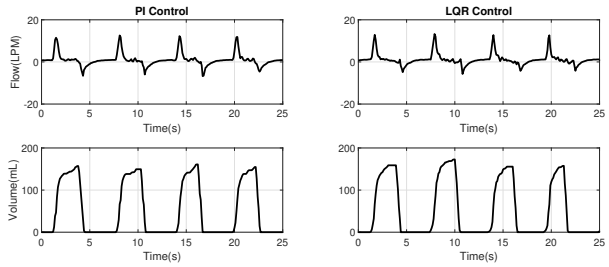

Fig. 8: Monitoring variables in pressure control.

The comparison of the controllers in the pressure support control mode is presented in Figure 9, in which a step type reference of Pressure with a magnitude of 15 cmH2O was also used. The response characteristics are as the same as the pressure control (see Table II).

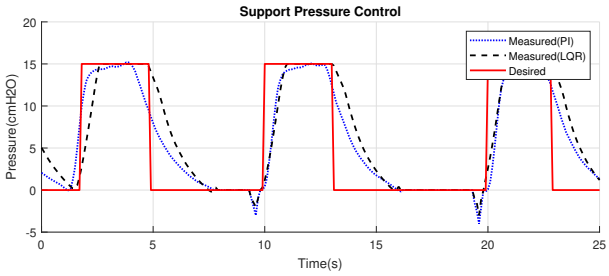

Fig. 9: PI vs LQR in pressure support control.

Both controllers were implemented on a NI myRIO Embedded Device (myRIO-1900).

IV. Conclusions

The focus of this work was to show the better performance of a LQR controller against a PI controller, specifically in medical applications, which is in this case is the generation of an air flow at a determined volume or pressure. Both control methods presented in this work were effective during the tracking of the desired parameters, where they showed good performance in terms of error, ensuring the stability of the controlled system.

Likewise, the results obtained from the LQR control compared to the PI control show a better performance with an error of 0.2% for the pressure control and 6.3% for the volume control. It is shown that the LQR method is a good option for the study and implementation of a controller for a

mechanical ventilation system, allowing it to be an attractive solution. However, it should be noted that the LQR controller performance was tested on an artificial lung. To test the robustness of the controller, it is recommended to use it in more complex structures that are more closely to a human lung in the experimentation process.

V. Acknowledgment

The authors would like to thank to cooperation agreement between Universidad de Ingenieria y Tecnologia - UTEC and Alta Engineering SAC - AE for making possible the development of the project.

References

[1] (2021) Who coronavirus (covid-19) dashboard. [Online]. Available: https://covid19.who.int/

[2] O. Bargain and U. Aminjonov, "Poverty and COVID-19 in Developing Countries," Groupe de Recherche en Economie Théorique et Appliquée (GREThA), Bordeaux Economics Working Papers 2020-08, Aug. 2020.

[3] M. Czajkowska-Malinowska, A. Kania, P. Kuca, J. Nasiłowski, S. Skoczyński, R. Sokolowski, and P. Śliwiński, "Treatment of acute respiratory failure in the course of covid-19. practical hints from the expert panel of the assembly of intensive care and rehabilitation of the polish respiratory society," *Advances in Respiratory Medicine*, vol. 88, pp. 245–266, 07 2020.

[4] G. Grasselli, E. Cattaneo, G. Florio, M. Ippolito, A. Zanella, A. Cortegiani, J. Huang, A. Pesenti, and S. Einav, "Mechanical ventilation parameters in critically ill covid-19 patients: a scoping review," *Critical Care*, vol. 25, 12 2021.

[5] Badre El Majid and Aboubakr El Hammoumi and Saad Motahhir and Ambar Lebbadi and Abdelaziz El Ghzizal, "Preliminary design of an innovative, simple, and easy to build portable ventilator for covid 19 patients," *Euro-Mediterranean journal for environmental integration*, no. 5, 2020.

[6] J. Pearce, "A review of open source ventilators for covid-19 and future pandemics," *F1000Research*, vol. 9, p. 218, 03 2020.

[7] A. Kwon, A. Slocum, D. Varelmann, and C. Nabzdyk, "Rapidly scalable mechanical ventilator for the covid-19 pandemic," *Intensive Care Medicine*, vol. 46, 06 2020.

[8] E. Calilung, J. Española, E. Dadios, A. Culaba, E. Sybingco, A. Bandala, R. Vicerra, A. Madrazo, L. Gan Lim, R. K. Billones, S. Lopez, D. D. Ligutan, J. Palingcod, and C. Castillo, "Design and development of an automated compression mechanism for a bag-valve-mask-based emergency ventilator," in *Health Care Devices and Intelligent Systems*, 12 2020, pp. 1–6.

[9] N. Bazán-Lavanda, E. A. Vela, R. Canahuire, J. Valdivia-Silva, and M. Palacios-Matos, "Solicitud de patente del ventilador mecánico de emergencia para uci," 2020.

[10] C. Rabec, D. Rodenstein, P. Leger, S. Rouault, C. Perrin, and J. Gonzalez-Bermejo, "Ventilator modes and settings during non-invasive ventilation: effects on respiratory events and implications for their identification," *Thorax*, vol. 66, no. 2, pp. 170–178, 2011.

[11] J. Masip, K. Planas, and A. Mas, *Non-invasive ventilation*. Springer, 02 2021, pp. 267–283.

[12] A. R. Moreno, *Control de Procesos Práctico y Avanzado*. Universidad Nacional de Ingeniería, 2012.

[13] M. P. Martin, "Economic model predictive controllers in a micro-grid with hydrogen storage," Ph.D. dissertation, School of Engineering, University of Seville, 2013.

[14] K. Ogata, *Modern Control Engineering*, 5th ed. Prentice Hall, 2010.

[15] J. G. Proakis and D. G. Manolakis, *Tratamiento digital de senales*. Pearson Educacion, 2010.